ISSN 0915-633X

NATIONAL INSTITUTE FOR FUSION SCIENCE

Spectrograph of Electric Field Fluctuation in Toroidal Helical Plasma

A. Fujisawa, K. Itoh, A. Shimizu, H. Nakano, S. Ohsima, H. Iguchi,
K. Matsuoka, S. Okamura, S.-I. Itoh and P. H. Diamond

(Received - Aug. 23, 2005)

NIFS-817

Sep. 2005

RESEARCH REPORT
NIFS Series

TOKI, JAPAN

Spectrograph of Electric Field Fluctuation in Toroidal Helical Plasma

A. Fujisawa, K. Itoh, A. Shimizu, H. Nakano, S. Ohsima, H. Iguchi, K. Matsuoka, S. Okamura, S.-I. Itoh[1] and P. H. Diamond[2]

National Institute for Fusion Science, Oroshi-cho, Toki-shi, 509-52 Japan
[1]RIAM, Kyushu Univ., Kasuga 816 Japan
[2]University of California, San Diego, La Jolla, California, United States of America

Abstract. This is a report on fluctuation measurements using twin heavy ion beam probes in CHS. The observation shows that a dozen of coherent modes with intermittent nature coexist in an electron cyclotron heated plasma. The modes are found to have long-distance correlation in toroidal direction. The radial structure of the modes are evaluated in potential fluctuation. The characteristics are not in contradictory with geodesic acoustic modes.

Keywords; electric field fluctuation, heavy ion beam probes, geodesic acoustic modes, long-range correlation, radial eigen function

1. Introduction

Research on magnetically confined plasmas has revealed that turbulence is a key to control cross-field transport and determine the structure of toroidal plasmas[1, 2, 3]. The causes of improved confinement modes or transport barriers following the discovery of H-mode[4] can be ascribed to the formation of radial electric field shear that should suppress the turbulence and the resultant transport. Then, the plasma transport is conventionally tried to be understood in the framework of relations between two major elements, *i. e.*, turbulence and mean radial electric field[5].

In addition to the two elements, recent development of theories and direct nonlinear simulations have suggested that zonal flow, mesoscopic structure of radial electric field, should be another element essential to explain plasma transport[6]. The zonal flows are generated from nonlinear interactions with turbulence, and the energy transfer from turbulence to zonal flows is one of the mechanisms to determine the saturation level of turbulence and resultant transport.

In toroidal plasma, the zonal flows emerge in electric field fluctuation symmetric ($m = n = 0$) on magnetic flux surface with finite radial wave numbers[7, 8]. Zonal flows are classified to two categories; one is a stationary branch characterized with slowly varying time-dependent ripple structure, and the other is a coherent oscillatory branch, Geodestic Acoustic Modes (GAM)[9, 10, 11, 12]. Recent CHS experiments confirmed the existence of stationary branch of zonal flow in direct measurements of radial electric field fluctuation using twin heavy ion beam probes

(HIBP)[13, 14], while coherent oscillations, probably GAMs, have been reported in many experiments[15, 16, 17, 18, 19, 20].

In the previous article of CHS, the presence of a coherent frequency mode at 16.7 kHz was briefly reported together with identification of the stationary zonal flows. The article presents the recent progress in the study of such coherent modes. The HIBPs detect coexistence of a dozen of coherent modes in the electron cyclotron resonance heated (ECRH) plasmas with a rather low density. Detailed analysis including an estimate of radial profiles of the modes shows that some of the modes are localized around the observation point, while the others sensed as path integrated fluctuations are somewhere along the beam orbit. The modes exhibit intermittent density and potential fluctuations that are well correlated with each other. The measurement of electric field fluctuation confirms that the modes have long-distance correlation between twin toroidal locations.

2. Compact Helical System and Heavy Ion Beam Probes

2.1. CHS and HIBPs

Compact Helical System (CHS) is a toroidal helical device of which the major and averaged minor radii are $R = 1$ m and $a = 0.2$ m, respectively. A pair of helical coils generates the confinement magnetic field that has m=2 and n=8 symmetry in poloidal and toroidal direction, respectively. Four pairs of poloidal field coils are equipped to control magnetic axis and to shape magnetic field cage, such as ellipticity and triangularity. Two neutral beam injection (NBI) systems and two gyrotrons are used as heating apparatus. Combination of these heating methods allows a wide choice of plasma parameters. CHS has two HIBPs located in different toroidal positions 90° apart. Each of the HIBPs is equipped with three channels to observe the adjacent spatial points of the plasma. The HIBP systems allow us to investigate local and global characteristics of turbulence.

2.2. Principles of HIBP measurements

Heavy ion beam probe is a synthetic diagnostics to measure local density, potential, and their fluctuations simultaneously[21, 22]. In the diagnostics, accelerated cesium beams of a singly ionized state are injected into the plasma. Doubly ionized beams produced through electron impact collisions in the plasma are detected with an energy analyzer. The energy difference between the injected and detected beams corresponds to the plasma potential at the ionization point. The fluctuation in detected beam intensity brings information of local density fluctuation at the ionization point. The fluctuation is expressed as a sum of the local density fluctuation and the integrated density fluctuation along the beam orbit, as

$$\delta I/I(r) = \delta n/n(r) - \int_r^a \delta n S_1 \mathrm{d}l_1 - \int_r^a \delta n S_2 \mathrm{d}l_2$$

where S_1 and S_2 are the ionization rates from singly charged and doubly charged ions to the higher charged ones, respectively. In a sufficiently low density plasma, the second and third terms can be neglected and the fluctuation should reflect local density fluctuation.

Similarly to the density fluctuation, the potential fluctuation is an integral of electric field fluctuation, which is expressed as

$$\delta\phi(r) = 2\int_r^a \delta E \mathrm{d}l_2 - \int_r^a \delta E \mathrm{d}l_1.$$

Therefore, the potential fluctuation can sense the electric field fluctuation along the beam orbit. Assuming the electric field fluctuation as $\delta E \delta l = \delta\phi_{\mathrm{local}}$, then the formula is reformed into

$$\delta\phi(r) = \delta\phi_{local} + \delta\phi_{\mathrm{path}} = \delta E \delta l + 2\int_{r-\delta r}^a \delta E \mathrm{d}l_2 - \int_{r-\delta r}^a \delta E \mathrm{d}l_1.$$

The potential at the neighboring observation point $\delta\phi(r-\delta r)$ is considered to be equivalent to $\delta\phi_{\mathrm{path}}$, therefore, the local fluctuation or electric field fluctuation can be evaluated from the combination of $\delta\phi(r) - \delta\phi(r-\delta r) = \delta\phi_{\mathrm{local}}$, that is, potential difference between two of the three local channels.

3. Coherent Modes in Electric Field Spectra

3.1. Experimental Conditions

The target plasma is produced with electron cyclotron resonance (ECR) heating of $\sim$ 200 kW, to measure purely electrostatic fluctuation with avoiding magneto-hydro-dynamic (MHD) behavior. The chosen plasma parameters were, magnetic field strength $B = 0.88$ T, density $n_{\mathrm{e}} \simeq 4 \times 10^{12}\mathrm{cm}^{-3}$, electron temperature $T_{\mathrm{e}} \simeq 1$ keV, and ion temperature $T_{\mathrm{i}} \simeq 0.1$ keV.

The twin HIBPs measurement was performed using cesium beam. The necessary beam energy is $\sim$70 keV for the experimental condition of the magnetic field strength. In this experimental condition, a good signal-to-noise ratio is obtained at the radial position of $r = 12$ cm or at the normalized minor radius $\rho \sim 0.6$, where the detected beam current takes the maximum. In addition, the position is usually free from the transition phenomenon, and provides a better condition in reproducibility.

Global characteristics of the turbulence can be inferred from the twin HIBP measurements. The observation point of an HIBP is changed to survey the structure of coherent modes, while the observation point of an HIBP is fixed at $r = 12$ cm to monitor variation of the mode intensity between discharges. The observation point was varied in every 1 mm within $\pm$2cm around $r \simeq 12$ cm.

3.2. Spectra and Local Fluctuation Characteristics

Figure 1 shows power spectra of density, potential and electric field fluctuations at the position of $r = 12$ cm in the frequency range from 5 to 100 kHz. Here, the normalized density fluctuation defined as $\delta n/n$ is displayed, where n is the temporal average of local density. The plotted spectra are the ensemble averages of more than forty shots, and elemental spectra are evaluated as the averages of $\sim$ 2 ms windows in a stationary period of $\sim$ 40 ms in a discharge duration of $\sim$ 100ms. A spectrum of a window including 2^{10} digital data is calculated using the Fast Fourier Transform (FFT) technique to give a frequency resolution of $\sim$ 0.48 kHz. The Nyguist frequency is 250 kHz for 2 μs sampling.

Several peaks are found to be superposed on broad-band spectra in both density and potential fluctuations; for density fluctuation the peaks are at the frequencies of 8, 16, 23, 35, 44, 50 and 125 kHz, while 8, 16, 18, 23, 29, 35, 44, 50 and 125 kHz for potential fluctuation. The spectrum of electric field fluctuation also shows peaks, however, the number of the countable peaks is reduced compared to that in the density and potential fluctuations. Since the density and potential fluctuations suffer from the path-integral fluctuations, the absence of the peaks in electric field fluctuation indicates that the corresponding modes should be localized somewhere along the beam orbit. On the other hand, the modes of the peak frequencies at 8, 16, 18, 35 and 50 kHz are localized around $r = 12$ cm. The noise level is plotted in the figures, and it is obvious that the noise level is sufficiently low to deduce the power of the coherent modes, even in the power of electric field fluctuation.

3.3. Local Dynamics of Coherent Modes

Simultaneous measurement shows that density and potential fluctuations are well-correlated at the frequency of the modes. Figure 2 illustrates coherence between density and potential fluctuations at the observation radius. In the frequency range from 20 to 100 kHz, the coherence shows significant value up to ~ 0.6 indicating broad band characteristics of turbulence. Local maxima of coherence are found at the frequencies of 8, 16, 18, 23, 35, (44), 50 and 125 kHz, corresponding to the peaks of density and potential fluctuation spectra. The phase relation between density and potential fluctuations is shown in Fig. 2b. The phase in the broad band turbulence has a finite value ($\sim 0.1\pi$), suggesting that fluctuation in this range should cause a certain amount of turbulence-driven particle flux. On the other hand, the phases at the peak frequencies indicate jumps from the phase of background turbulence which continuously changes as frequency.

The dynamics of the modes can be extracted using numerical filter defined as $\bar{x}(t) = \int_{-\infty}^{\infty} w(t-t')x(t')dt'$ with $w(t) = (\sin 2\pi f_h t - \sin 2\pi f_l t)/\pi t$ where f_h and f_l are the cut-off frequencies for higher and lower boundaries, respectively. Figure 3 shows, for an example, the waveforms of density and potential for the sharpest peak at 8 kHz, where the cut off frequencies are chosen as $f_l = 5$ kHz and $f_h = 10$ kHz. The waveform in a long time scale indicates intermittent nature of the mode. The life time of the burst is ~ 500 μs, corresponding to the width of the peak about ~ 0.35 kHz (see Fig. 3b). The inset is an expanded view of the waveform to demonstrate the phase difference between density and potential. The phase between them is seemingly consistent with the result of Fourier analysis ($\sim 0.3\pi$), although a slight time-variation in the phase can be seen for the waveform.

As the ratio of the background turbulence to a coherent mode turns larger, it becomes difficult to obtain a definite phase relation between the density and potential fluctuations of the modes due to the contamination of turbulence contribution. Particularly for the coherent mode with a long correlation length, the path integral contribution could disturb the local phase relationship between density and potential fluctuations. For the peak of 125 kHz, the density fluctuation comes from the path integrated contribution, hence, the phase difference between the local density and electric field can be shifted by π to the observed phase. Besides, an attention should be paid on the fact that a statistical analysis simply assuming stationariness of the mode may just give a temporal averaged phase without regard to the intermittent nature of the modes.

3.4. Global Characteristics of Fluctuations

Utilizing twin HIBP signals, the coherence between fluctuations at two toroidal locations are calculated in three manners; (1) coherence between potential fluctuations, (2) that between electric field and potential fluctuations, and (3) that between electric field fluctuations. Figure 4 shows the shot-averaged coherences for the above three cases. Note that the plotted coherence values are obtained in a condition that one of the HIBP observation points is varied in a radial extent of ± 2 cm around $r = 12$ cm.

In the first case, the local maxima corresponding to the peaks of the potential spectrum are found to have the highest values among the three cases of coherence. Surprisingly, a long-distance correlation is found even in the highest frequency peak at 125 kHz in potential-potential correlation. In the second case, the coherence at the peaks decrease and some of the peaks are lost in the background level. In particular, the two peaks are clearly distinguished around the frequency of 17 kHz, demonstrating the presence of two different modes in the narrow frequency range. This reduction of the coherence and the disappearance of peaks can be ascribed to the loss of the path integral term, therefore, the degree of reduction may give a rough idea of the radial extent of the mode localization. The complete disappearance of the peak means that the mode of ~ 125 kHz is localized outside $r = 12$ cm. Finally, in the third case the four peaks at 8, 16, 18 and 35 kHz can be still recognized although the absolute values of coherence are extremely reduced. The radial extent of these four modes should, therefore, contain the observation point.

A cause of the small coherence between electric fields should be the poor signal-to-noise ratio of one of the HIBP signal; about 2/3 for the mode at 8kHz. The Fourier coefficients of the signals are supposed to be expressed as $F_a = F_{a0}$ and $F_b = F_{b0} + F_{\rm noise}$. Then, the coherence can be written as $\gamma_N = |P_{\rm cr}|/\sqrt{P_a \cdot P_b} \sim \gamma_c/\sqrt{1+\alpha}$, where $\alpha = P_{\rm noise}/P_{\rm b0}$, $\gamma_c = |P_{\rm cr}|/\sqrt{P_{\rm a0}P_{\rm b0}}$, $P_a = |F_a|^2$, $P_b = |F_b|^2 = |F_{b0}|^2 + |F_{\rm noise}|^2$, $P_{\rm noise} = |F_{\rm noise}|^2$ and $P_{\rm cr} = \langle F_{a0}F_{b0}\rangle$, where $\langle\rangle$ means the statistical average of ensemble. For the mode at 8 kHz, the corrected coherence can be estimated to be $\gamma_c \sim 0.45$ from the experimental result of $\gamma_N \sim 0.3$. An increment in the signal-to-noise ratio may provide a significant phase relation between two toroidal locations in electric field fluctuations. Then, the symmetry of the modes can be investigated in local measurements.

3.5. Radial Structure of Coherent Modes

The radial structure of the coherent modes can be inferred by varying an observation point shot by shot, with the other observation points being fixed as the reference to correct the variation of the mode intensity between shots. Figure 5 shows the potential fluctuation powers of four modes at 8, 16, 18 and 35 kHz as a function of radius. In the analysis, the fluctuation power is once normalized by the reference, then the normalized value is converted into dimension of power by multiplying the shot-averaged power of the mode for the analysed set of discharges.

Obviously from Fig. 5a, the power of the lowest frequency mode at 8 kHz increases toward the edge, while that of the other higher mode at 35 kHz increase toward the core where the electron temperature is higher. On the other hand, the power profiles at the frequencies of 16 and 18 kHz is shown in Fig. 5b. The power at 16 kHz has a maximum around $r = 12$ cm, while the other increases toward the plasm core. This difference in the radial profile supports the hypothesis that the fluctuations at these

frequencies should be ascribed to the two different modes, as is expected from the spectrum of the local potential fluctuation and the global coherence analysis, though in a quite narrow frequency range.

4. Discussion and Summary

The coherent modes show eigen-mode characteristics with a long distance correlation in a toroidal location. These characteristics of the modes suggest that the modes could be Magneto-hydro-dynamic (MHD) modes, or GAMs. However, clear coherence is not found between potential and magnetic field fluctuations from Mirnov coils. The tendency that location of modes with higher frequency moves inward to the region of higher temperature should be consistent with dependence of the GAM frequency as the theories expect; *i. e.*, $\omega_{\rm GAM} \sim c_{\rm s}/R \propto \sqrt{T_e}$, where c_s, R and $T_{\rm e}$ are the ion sound velocity, the major radius and the electron temperature, respectively. However, the following three issues, at least, should be confirmed to definitely verify that some of the modes should be really GAMs; the axi-symmetry (m=n=0) of electric field fluctuation, the asymmetry (m=1/n=0) of density fluctuation, and a significant causal relation of the modes with the background turbulence. Twin HIBP measurements can address these three issues for future experiments. The third point, the causal relation, can be investigated with a help of bicoherence analysis that can reveal three-wave couplings[20].

In summary, the spectrograph of density and potential fluctuations with HIBPs have shown coexistence of almost a dozen of coherent modes in ECR-heated plasma. Several basic characteristics are identified for these modes; well-correlated density and potential fluctuations with the intermittent or time-dependent nature, the radial distribution of the modes, the long-distance correlation in toroidal direction, and eigen mode property. As for some of the significantly coherent modes, the radial distribution shows a tendency that higher frequency modes are placed in a higher temperature regime. The characteristics of the modes are not contradictory with those of GAMs, although complete identification should await future experiments.

Acknowledgements

This work is partly supported by the Grant-in-Aids for Scientific Research (No. 15360497) and Specially-Promoted Research (No.16002005). The authors are grateful to Prof. O. Motojima for his continuous supports and encouragements.

References

[1] A. Yoshizawa, S. -I. Itoh, K. Itoh, *Plasma and Fluid Turbulence* (Institute of Phys. Pub., Bristol and Philadelphia, 2003).
[2] H. Biglari, P. H. Diamond, P. W. Terry, Phys. Fluids B **2** 1 (1990).
[3] K. Itoh, S.-I. Itoh, A. Fukuyama, H. Sanuki, M. Yagi, Plasma Phys. Control. Fusion **36** 123 (1994).
[4] F. Wagner et al., Phys. Rev. Lett. **49** 1408 (1982).
[5] A. Fujisawa, Plasma Phys. Control. Fusion **45** R1 (2003).
[6] M. N. Rosenbluth, F. L. Hinton, Phys. Rev. Lett. **80**, 724 (1998).
[7] P. H. Diamond, Y. -M. Liang, B. A. Carreras, P. W. Terry, Phys. Rev. Lett. **72** 2565 (1994).
[8] P. H. Diamond, K. Itoh, S.-I. Itoh, T. S. Hahm, Plasma Phys. Control. Fusion **47** R35 (2005).
[9] N. Winsor, J. L. Johnson, and J. M. Dawson, Phys. Fluids 11, 2448 (1968).
[10] K. Hallatschek, D. Biskamp, Phys. Rev. Lett. **86** 1223 (2001).
[11] T. Watari, Y. Hamada, A. Fujisawa, K. Toi, K. Itoh, Phys. of Plasmas **12** 062304 (2005).
[12] K. Itoh et al., Phys. of Plasmas in press.

[13] A. Fujisawa et al., Phys. Rev. Lett. **93** 165002 (2004).
[14] G.S. Xu et al., Phys. Rev. Lett. 91, 125001 (2003)
[15] P. M. Schoch, K. A. Connor, D. R. Demers, X. Zhang, Rev. Sci. Intrum. **74** 1846 (2003).
[16] M. G. Shats, W. M. Solomon, Phys. Rev. Lett. **88**, 045001 (2002).
[17] G. R. McKee, *et al.*, Plasma Phys. Control. Fusion **45**, A477 (2003).
[18] Y. Hamada, A. Nishizawa, T. Ido et al., Nucl. Fusion **45** 81 (2004).
[19] T. Ido et al., submitted to Nucl. Fusion.
[20] Y. Nagashima et al., Phys. Rev. Lett. in press.
[21] A. Fujisawa, *et al.* Rev. Sci. Instrum. **67**, 3099 (1996).
[22] T. P. Crowley, IEEE Trans. Plasma Sci. **22** 291 (1994).

Figure 1. Spectra of (a) density, (b) potential and (c) electric field fluctuations in an ECR-heated plasma. The observation point is $r = 12$ cm, where the signal-to-noise ratio for HIBP measurement is maximum for the operational condition. The noise levels are about $2\times10^{-8}\mathrm{kHz}^{-1}$ $1\times10^{-8}\mathrm{kV}^2/\mathrm{kHz}$ and $2\times10^{-8}\mathrm{kV}^2/\mathrm{kHz}$ for density, potential and electric field fluctuations, respectively.

Figure 2. (a) Coherence and (b) phase between density and potential fluctuations. The significant coherence can be found at the peaks in density and potential fluctuations in Figs. 1.

Figure 3. (a) Waveforms of potential fluctuation around the peak at 8 kHz. The signal is band-pass filtered numerically in the frequency range from 5 to 10 kHz. The inset shows filtered density (solid line) and potential (dashed line) fluctuations, indicating delay of the potential signal to the density. (b) An expanded view of electric field fluctuation spectra around the peak frequency. The Gaussian fitting of $\exp(-(f - f_0)^2/2\Delta f^2)$ gives the results of $\Delta f = 0.35$ kHz and $f_0 = 8.3$ kHz. Intermittent nature is seen in the signals with a life time consistent with the width of the peak in the spectrum.

Figure 4. Coherence between fluctuations at two toroidal locations. The solid, grey-dashed and the black-dashed lines represent the curves of coherence between electric field fluctuations, electric field-potential fluctuations, and potential-potential fluctuations at two toroidal locations. Four peaks are identical even in the coherence between electric field fluctuations.

Figure 5. Potential fluctuation powers of the four coherent modes as a function of radius. (a) The powers at 8kHz and 35 kHz, and (b) the powers at twin peaks of 16 and 18 kHz. The different characteristics of these two frequencies mean existence of two individual modes in the narrow frequency range. A tendency is found that the higher frequency modes are localized in higher temperature region.

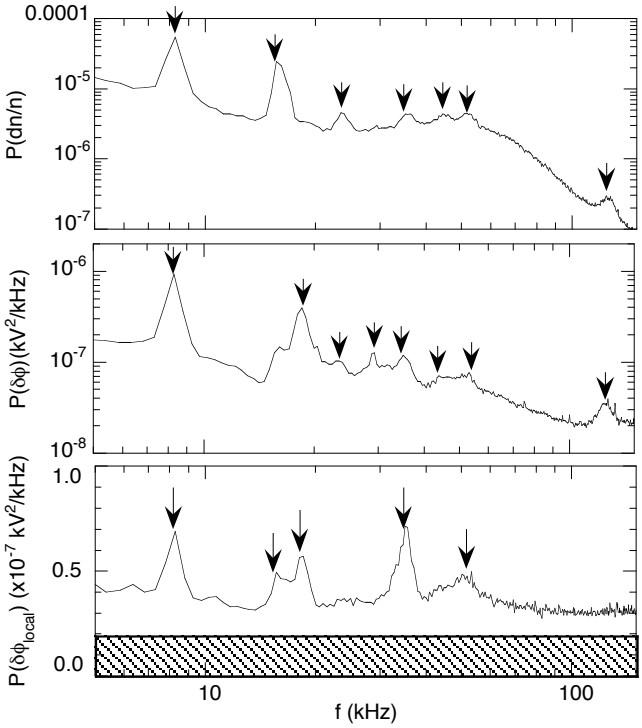

Figure 1 A. Fujisawa

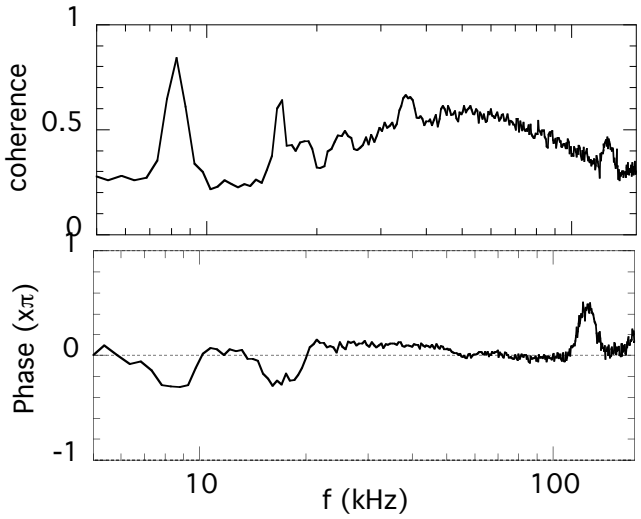

Figure 2 A. Fujisawa

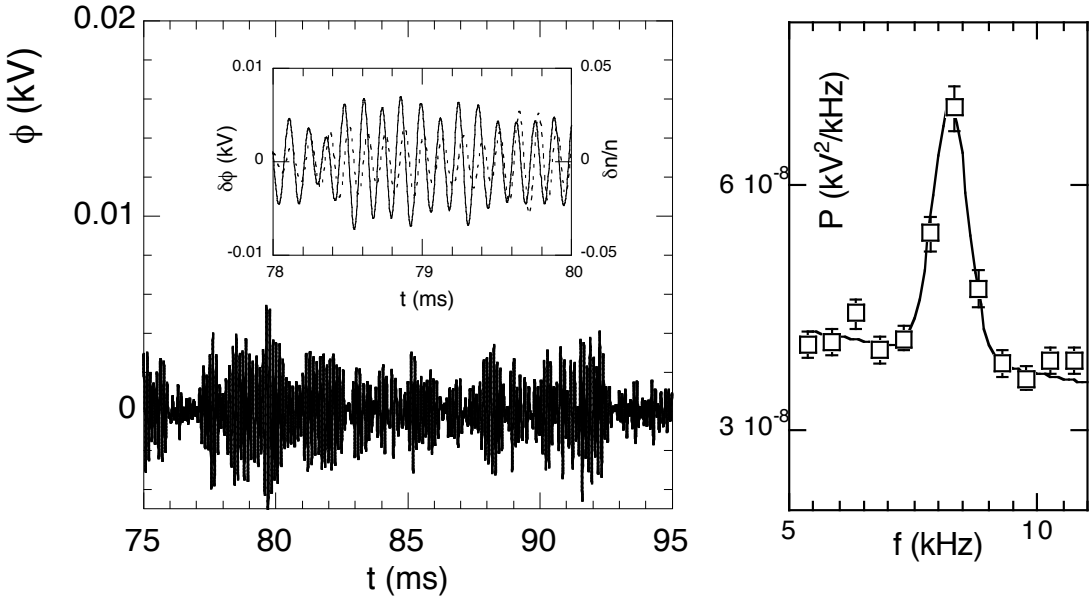

Figure 3 A. Fujisawa

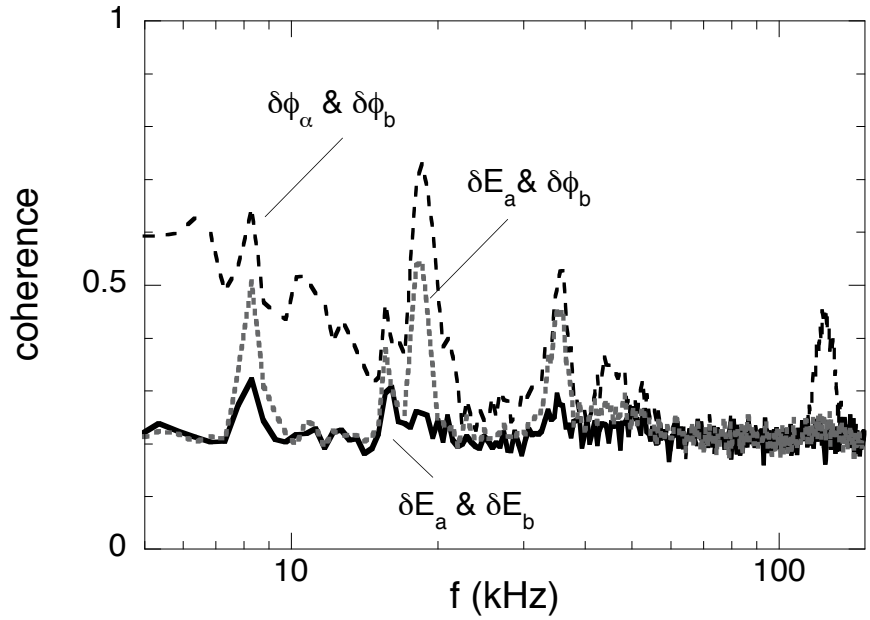

Figure 4 A. Fujisawa

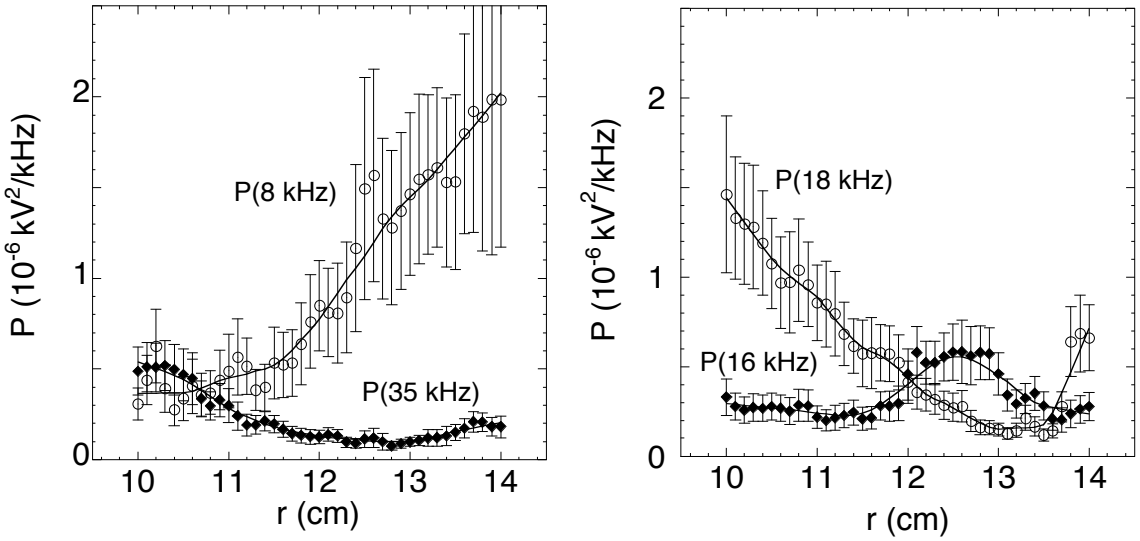

Figure 5. A. Fujisawa